Ultrafast Photoinduced Insulator-Ferromagnet Transition in the Perovskite Manganite $Gd_{0.55}Sr_{0.45}MnO_3$

M. Matsubara,[1,*] Y. Okimoto,[1] T. Ogasawara,[1] Y. Tomioka,[1] H. Okamoto,[1,2] and Y. Tokura[1,3,4]

[1]*Correlated Electron Research Center (CERC), National Institute of Advanced Industrial Science and Technology (AIST), Tsukuba 305-8562, Japan*

[2]*Department of Advanced Materials Science, University of Tokyo, Chiba 277-8561, Japan*

[3]*Department of Applied Physics, University of Tokyo, Tokyo 113-8656, Japan*

[4]*Multiferroics Project, ERATO, Japan Science and Technology Corporation, AIST Tsukuba Central 4, Tsukuba 305-8562, Japan*

(Received 16 February 2007; published 15 November 2007)

We have investigated the ultrafast spin and charge dynamics in the course of a photoinduced phase transition from an insulator with short-range charge order and orbital order (OO) to a ferromagnetic metal in perovskite-type $Gd_{0.55}Sr_{0.45}MnO_3$. Transient reflectivity changes suggest that the metallic state is formed just after the photoirradiation and decays within ~1 ps. The magnetization, however, increases with the time constant of 0.5 ps and decays in ~10 ps. The relatively slow increase of the magnetization is attributable to the magnetic-field-induced alignment of ferromagnetic domains in the initially produced metallic state and its slow decay to the partial recovery of the OO.

DOI: 10.1103/PhysRevLett.99.207401 PACS numbers: 78.20.Ls, 75.25.+z, 75.47.Lx, 78.47.+p

New methods for control of the magnetization by other than magnetic fields are strongly desired from fundamental and technological viewpoints [1–3]. Recent developments in femtosecond (fs) laser technology provide a promising route to ultrafast control of magnetization [4]. In most cases, however, the observed changes of magnetization are the photoinduced demagnetization as a result of rapid temperature increase of the spin system. This is because a spin state can hardly be changed by optical excitation due to the selection rule. Nevertheless, several attempts for the nonthermal optical control of magnetization were successfully performed: for example, the generation of a ferromagnetic order by photogenerated carriers in paramagnetic (In, Mn)As/GaSb heterostructure [5], the excitation of coherent magnons coupled with optical phonons at a ferromagnetic Gd surface [6], and the ultrafast coherent control of magnetization by way of the inverse Faraday effect in a weak ferromagnet $DyFeO_3$ [7].

In the present study, we investigate another way of nonthermal optical control of magnetization on an ultrafast time scale. A key strategy is to utilize the phase competition between antiferromagnetic and ferromagnetic states [8]. Typically in a correlated electron system, the strong coupling among spin, charge, and orbital degrees of freedom of electrons will make it possible to control magnetic properties via cooperative effects induced by optical excitation. A material appropriate for this purpose is a perovskite manganite, $R_{1-x}A_xMnO_3$ (R: rare-earth ion, A: alkaline-earth ion). Around $x = 0.5$ the charge and orbital-ordered insulator (CO-OOI) phase accompanied with the antiferromagnetic (AF) spin state is observed in a number of manganites in common, and competes with the ferromagnetic metallic (FM) phase stabilized by the double-exchange (DE) interaction [9]. Recently, several attempts to achieve the photoinduced CO-OOI to FM transition have been made on the manganites [10,11]. In fact, the CO-OOI to metal transitions have been reported in $Pr_{0.55}(Ca_{1-y}Sr_y)_{0.45}MnO_3$ thin film [12] and $Gd_{0.55}Sr_{0.45}MnO_3$ single crystal [13] located near the boundary between CO-OOI and FM phases. The photoinduced magnetizations, however, have not been investigated in these materials.

As a candidate for the investigation of the ultrafast spin dynamics in the CO-OOI to FM transition, we adopt $Gd_{0.55}Sr_{0.45}MnO_3$. Figure 1(a) shows the phase diagram of the $R_{0.55}Sr_{0.45}MnO_3$ series as a function of the averaged ion radius r_A of the A site ($R_{0.55}Sr_{0.45}$) ions [14]. The compounds with $r_A > 1.32$ Å are in the FM phase below the critical temperature T_C. With decrease of r_A, the one-

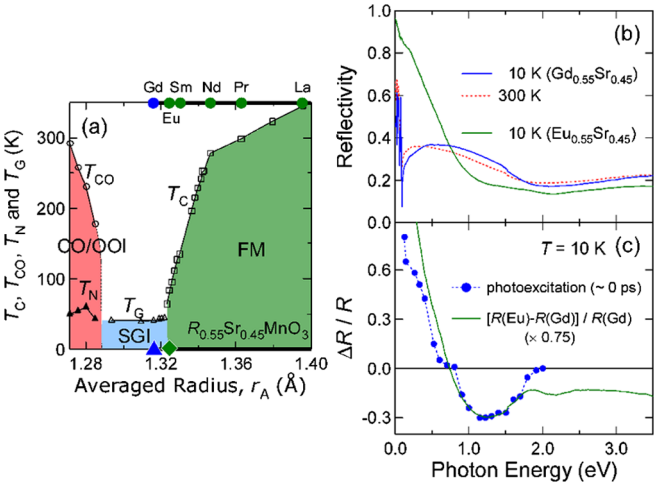

FIG. 1 (color online). (a) The phase diagram consisted of mainly $R_{0.55}Sr_{0.45}MnO_3$ series [14]. (b) Reflectivity spectra of $Gd_{0.55}Sr_{0.45}MnO_3$ and $Eu_{0.55}Sr_{0.45}MnO_3$. (c) The differential reflectivity spectrum $\Delta R/R$ just after photoexcitation (~0 ps, circles) and the numerical one $[R(\mathrm{Eu}) - R(\mathrm{Gd})]/R(\mathrm{Gd})$ (solid line) at 10 K.

electron bandwidth is decreased and the quenched disorder is enhanced due to the large difference of the ionic radius between Sr^{2+} and R^{3+}, resulting in the destabilization of the FM phase as observed in the decrease of T_C. When $r_A < 1.32$ Å, the FM phase disappears. Instead, the spin glass insulator (SGI) phase with short-range CO-OO appears below the spin glass transition temperature T_G, e.g., in $Gd_{0.55}Sr_{0.45}MnO_3$ ($T_G = 44$ K) [the triangle in Fig. 1(a)]. As shown in Fig. 1(b), the reflectivity spectrum in $Gd_{0.55}Sr_{0.45}MnO_3$ characteristic of CO-OOI changes to the metallic one in $Eu_{0.55}Sr_{0.45}MnO_3$ locating on the left edge of the FM region [the diamond in Fig. 1(a)].

Recent pump-probe (PP) reflection spectroscopy on $Gd_{0.55}Sr_{0.45}MnO_3$ has revealed that a large reflectivity change ($\Delta R/R$) over a wide energy region was induced by a fs photoexcitation [the solid circles in Fig. 1(c)] [13]. The $\Delta R/R$ spectrum right after the photoexcitation is similar to the differential reflectivity spectrum between those for $Gd_{0.55}Sr_{0.45}MnO_3$ and $Eu_{0.55}Sr_{0.45}MnO_3$ at 10 K [the solid line in Fig. 1(c)]. This suggests that the CO-OO is melted and the metallic state is produced within the time resolution [13]. To confirm photoinduced ferromagnetism and clarify the spin-charge correlation in the photoinduced transition, it is necessary to detect the spin dynamics as well as the charge dynamics on an ultrafast time scale. In this Letter, we report on the time-resolved magneto-optical Kerr effect (TRMOKE) in $Gd_{0.55}Sr_{0.45}MnO_3$. By comparing the magnetization dynamics with the charge dynamics, we discuss the microscopic mechanism of the photoinduced CO-OOI to FM phase transition.

A single crystal of $Gd_{0.55}Sr_{0.45}MnO_3$ with pseudocubic perovskite structure was grown by a floating zone method [14]. A specimen cut from the crystal rod was polished and annealed at 1000 °C in oxygen atmosphere for optical measurements. For the fs PP spectroscopy, a Ti:sapphire regenerative amplifier with the wavelength of 800 nm (1.55 eV), the pulse width of 100 fs, and the repetition of 1 kHz was used as the light source. The output of the amplifier was divided into two beams: one was used for the pump light and the other was frequency doubled (3.1 eV) and used for the probe light. The spot diameters of the pump and probe light are 1.1 and 0.28 mm, respectively. At 3.1 eV, the static Kerr rotation angle θ_{Kerr} reaches the maximum, reflecting the magnetization of the manganites, as demonstrated in $La_{0.6}Sr_{0.4}MnO_3$ [15]. In fact, it was ascertained that the temperature variation of θ_{Kerr} at this energy is very similar to that of the magnetization. In the TRMOKE measurements, the polarization change $\Delta\theta$ of the reflected probe light from the sample is detected by a balanced detection technique. A magnetic field of ~0.25 T was applied normal to the sample surface. The photoinduced Kerr rotation change $\Delta\theta_{\mathrm{Kerr}} = \frac{1}{2}[\Delta\theta(M) - \Delta\theta(-M)]$ was measured by changing the sign of the magnetic field to eliminate the contribution from the pump induced optical anisotropy. The schematic of the experiment is shown in the inset of Fig. 2(d). We also measured transient reflectivity change $\Delta R/R$ at 0.12 eV as well as at 3.1 eV and used it as a probe of charge dynamics. The probe light at 0.12 eV was generated by using an optical parametric amplifier.

First, to see the photoinduced charge dynamics, in Figs. 2(a) and 2(b) we show the time evolutions of $\Delta R/R$ at 10 K, which were probed at 0.12 and 3.1 eV. The excitation density of the pump pulse is 0.42 mJ/cm^2 (~0.01 photons/Mn site). At 0.12 eV, the time profile consists of two components: the ultrafast component within 1 ps and the slower one dominating $\Delta R/R$ from 1 to 40 ps. The time profile at 3.1 eV also seems to include two components with the similar time constants, although the sign of the ultrafast component is negative. The small oscillatory signal on $\Delta R/R$ with the period of ~10 ps is attributable to an acoustic shock wave transmitting from the surface into the inside bulk [11]. To analyze these components, the data at 0.12 eV were fitted by the sum of the two exponential functions with the decay times τ_1 and τ_2, $I(t) = I_1 e^{-t/\tau_1} + I_2(1 - e^{-t/\tau_1})e^{-t/\tau_2}$. In Fig. 2(a), the fast and slow components obtained by taking into account the response function of the measurement system, and the sum of the two components are represented by the dotted, broken, and solid lines, respectively. The first component rises within the time resolution (~200 fs) and decays with $\tau_1 = 0.25$ ps, and the second one shows a gradual increase following the decay of the first component and then decays with $\tau_2 = 4.3$ ps. The first and second components are attributable to the photoinduced formation and decay of the metallic state and the electron-lattice thermalization process, respectively [13]. A reverse sign of $\Delta R/R$ in the first component for 0.12 and 3.1 eV is the expected one for the FM component, as seen in Figs. 1(b) and 1(c).

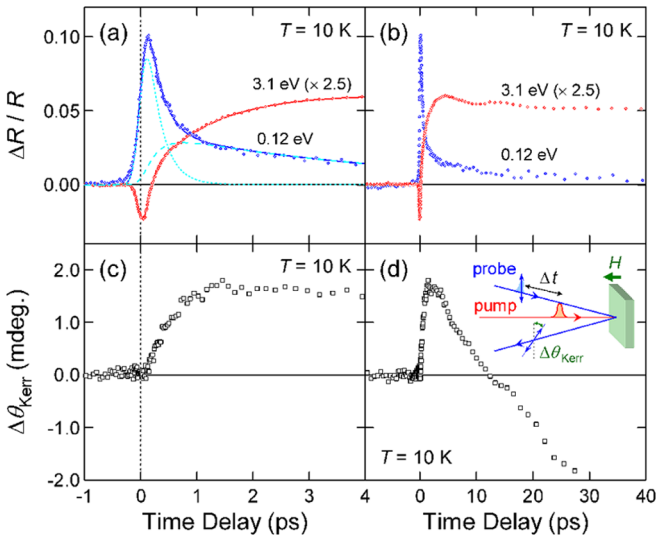

FIG. 2 (color online). Time evolutions of $\Delta R/R$ at 0.12 and 3.1 eV (a),(b) and $\Delta\theta_{\mathrm{Kerr}}$ at 3.1 eV at 10 K (c),(d). The excitation density is 0.42 mJ/cm^2 in common. In (a), the solid, dotted, and broken lines show the result of fitting (see text). The schematic of TRMOKE is shown in the inset of (d).

Next, we discuss the spin dynamics. In Figs. 2(c) and 2(d), the time evolutions of $\Delta\theta_{\mathrm{Kerr}}$ are presented. The excitation density (0.42 mJ/cm^2) is the same as that in the $\Delta R/R$ measurements. In the figures, the positive and negative $\Delta\theta_{\mathrm{Kerr}}$ signals correspond to the increase and decrease of the polar component of the magnetization, respectively. As seen in Fig. 2(c), $\Delta\theta_{\mathrm{Kerr}}$ rapidly increases upon the photoexcitation, indicating the increase of the magnetization with the rise time of 0.5 ps. Judging from the temperature dependence of the magnetization measured with the field-cooled (FC) run under 0.25 T shown in Fig. 4(a), the increase of the magnetization should be attributed not to photoinduced heating, but to a purely electronic process [16]. After the rapid increase, $\Delta\theta_{\mathrm{Kerr}}$ recovers to zero within ~10 ps, and then further decreases, being negative for the delay time $t_d > 10$ ps [Fig. 2(d)]. It is reasonable to consider that the rapid increase and subsequent (<10 ps) decrease of $\Delta\theta_{\mathrm{Kerr}}$ (the fast component) are associated with the generation of the ferromagnetic state and its recovery to the antiferromagnetic state. The negative $\Delta\theta_{\mathrm{Kerr}}$ (the slow component) is likely due to the demagnetization by the spin-lattice thermalization. As for the latter, note that the magnetization $M \approx 0.3\ \mu_B$/Mn is originally present at 10 K under 0.25 T [see Fig. 4(a)]. The static θ_{Kerr} in this condition is roughly evaluated to be ~15 mdeg by taking account of the fact that in the ferromagnetic manganite such as $La_{0.6}Sr_{0.4}MnO_3$ the magnetization of $4\mu_B$/Mn causes θ_{Kerr} of ~0.2 deg at 3.1 eV [15]. The observed negative $\Delta\theta_{\mathrm{Kerr}}$ of ~6 mdeg corresponds to the reduction of 40% of the magnetization by the photoirradiation.

Figures 3(a) and 3(b) show the time evolutions of $\Delta\theta_{\mathrm{Kerr}}$ at 10 K for different excitation densities on short (~5 ps) and longer (~2 ns) time scales, respectively. With increasing the excitation density, the fast positive component increases, suggesting that the photogenerated FM region becomes larger. The slow negative component also increases with the excitation density. In Figs. 3(c) and 3(d), we show the time evolutions of $\Delta\theta_{\mathrm{Kerr}}$ for 0.42 mJ/cm^2 at different temperatures. As the temperature is increased from 10 K, both the fast and slow components become smaller, and finally disappear. To investigate the temperature dependence in detail, we show the maximum (positive or negative) values of $\Delta\theta_{\mathrm{Kerr}}$ for the *fast* and *slow* components as a function of temperature in Figs. 4(b) and 4(c), respectively. The fast component grows up from a slightly higher temperature than T_G and gradually increases toward low temperatures. This suggests that the onset temperature of the photoinduced ferromagnetic order is related with T_C for the FM compound locating near the SGI-FM boundary [see Fig. 1(a)]. Comparing the magnitude of θ_{Kerr} (~0.2 deg) in $La_{0.6}Sr_{0.4}MnO_3$ with $\Delta\theta_{\mathrm{Kerr}} \sim 1.7$ mdeg for 0.42 mJ/cm^2 in $Gd_{0.55}Sr_{0.45}MnO_3$, we can see that the polar component of the magnetic moment is about 1% of the full moment, although the metallic state is formed immediately after the photoexcitation. As seen in Figs. 3(d) and 4(c), the values of $\Delta\theta_{\mathrm{Kerr}}$ are almost saturated for $t_d > 100$ ps, indicating that the magnetization is fully thermalized within 100 ps. The temperature variation of the slow component is similar to the thermally induced change of the magnetization, $\Delta M = M(T + \Delta T) - M(T)$ [the solid line in Fig. 4(c)], ensuring that the slow demagnetization process occurs through the thermalization of the spin system.

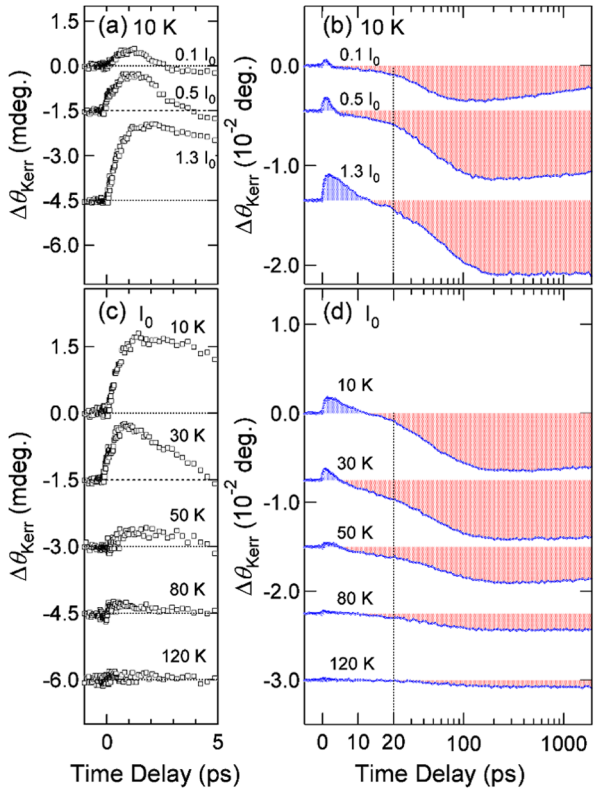

FIG. 3 (color online). Time evolutions of $\Delta\theta_{\mathrm{Kerr}}$ at 10 K for different excitation densities (a),(b) and for $I_0 = 0.42$ mJ/cm^2 at different temperatures (c),(d).

On the basis of the results, the photoinduced magnetization or demagnetization processes [Fig. 4(d)] can be interpreted as follows. First, the photocarriers melt the CO-OO and the metallic state is formed within the time resolution (~200 fs) [13], as observed in $\Delta R/R$ shown in Fig. 2(a). It should be noted that the ferromagnetic spin arrangement and the metallic behavior are strongly tied via the DE interaction in the manganites [9]. Namely, the ferromagnetic spin arrangements are indispensable for the formation of a metallic state. However, $\Delta\theta_{\mathrm{Kerr}}$ is never detected at this stage as shown in Fig. 2(c). This suggests that at the initial stage the magnetization of the photogenerated FM domains in the host of the spin glass state are randomly oriented and that the macroscopic magnetization is almost zero. Such a photoinduced state can be viewed macroscopically as a ferromagnetic cluster glass composed of the microscopic FM domains [the left panel of Fig. 4(d)]. At the second stage, the increase of $\Delta\theta_{\mathrm{Kerr}}$ occurs through the rotation of the microscopic FM domains toward a magnetic field direction with the time constant of 0.5 ps [the central panel

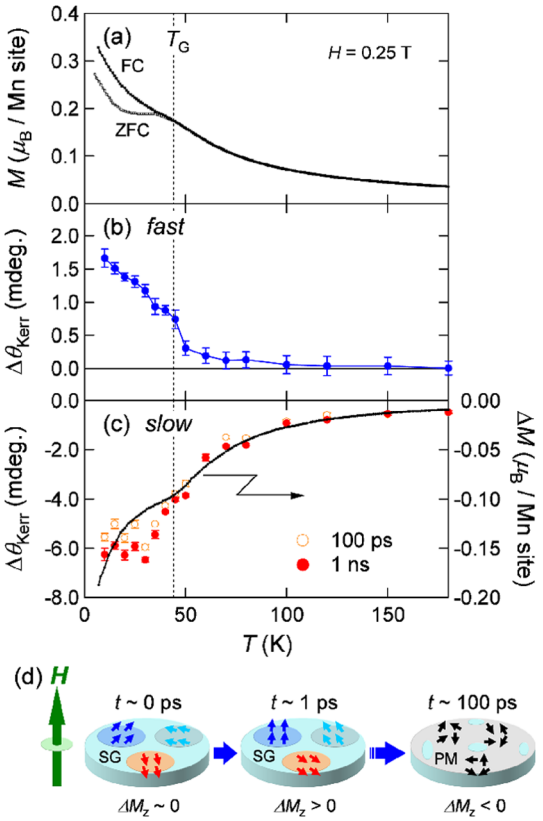

FIG. 4 (color online). (a) Temperature dependence of magnetization measured with zero-field-cooled (ZFC) and field-cooled (FC) runs under 0.25 T. (b),(c) Temperature dependence of (b) *fast* and (c) *slow* components of $\Delta\theta_{\mathrm{Kerr}}$ at 100 ps and 1 ns for 0.42 mJ/cm^2. The maximum value of the fast component ($\Delta\theta_{\mathrm{Kerr}} \sim 1.7$ mdeg) corresponds to about 1% of the full moment. The thermally induced change of magnetization, $\Delta M = M(T + \Delta T) - M(T)$ with $\Delta T = 50$ K, is shown by the solid line in (c). (d) The schematics of ultrafast ferromagnetism and subsequent demagnetization processes.

of Fig. 4(d)]. Here, we should note that the metallic state initially produced decays with 0.25 ps. It is, therefore, natural to consider that the ferromagnetic spin alignment at this stage is not completed. As a result, the observed $\Delta\theta_{\mathrm{Kerr}}$ is small. Subsequently, the ferromagnetic spin arrangement returns to the antiferromagnetic one after about 10 ps [see Fig. 2(d)]. Meanwhile, the ferromagnetic insulating state, which is perhaps stabilized by OO, is formed in the time region of ~0.3 to 10 ps. Finally, $\Delta\theta_{\mathrm{Kerr}}$ is further decreased with a time constant of ~50 ps for $t_d >$ 10 ps through the increase of the temperature of the spin system. Thus, the transition to the paramagnetic (PM) state occurs [the right panel of Fig. 4(d)].

An important feature of the present photoinduced transition is that the ferromagnetic spin arrangement occurs very fast. A possible scenario is as follows: the photoirradiation generates the charge excitation from Mn^{3+} to Mn^{4+}, which will destruct the CO and make the charges delocalized. In the delocalized state the DE interaction will make spins align ferromagnetically. As described in Ref. [13], the time scale of the formation of the FM state is expected to be ~20 fs when we assume the effective energy for the DE interaction to be ~0.2 eV. Subsequently, the alignment of ferromagnetic domains also occurs very fast (0.5 ps). Such a surprisingly fast rotation process of the magnetization might be explained by the enhanced magnetic resonance energy (or the $k = 0$ magnon frequency) of the FM domains as exchange biased by the adjacent antiferromagnetic region [17].

In summary, we demonstrated the ultrafast photoinduced ferromagnetism in a perovskite manganite, $Gd_{0.55}Sr_{0.45}MnO_3$. The microscopic FM state is photogenerated within 200 fs through the double-exchange interaction, while the macroscopic FM state is formed in 0.5 ps. Such an ultrafast photocontrol of magnetism based on the switched-on double-exchange interaction as well as the enhanced magnetic resonance energy may provide a useful basis for the future spintronics.

We thank I. Kézsmárki for reflectivity measurements and S. Ishihara for fruitful discussions. This work was partly supported by a Grant-In-Aid for Scientific Research (Grants No. 15104006, No. 17340104, and No. 16076205) from the MEXT, Japan.

*m-matsubara@aist.go.jp

[1] A. Asamitsu *et al.*, Nature (London) **388**, 50 (1997).
[2] H. Ohno *et al.*, Nature (London) **408**, 944 (2000).
[3] T. Lottermoser *et al.*, Nature (London) **430**, 541 (2004).
[4] E. Beaurepaire *et al.*, Phys. Rev. Lett. **76**, 4250 (1996); J. Hohlfeld *et al.*, *ibid.* **78**, 4861 (1997); A. Scholl *et al.*, *ibid.* **79**, 5146 (1997); B. Koopmans *et al.*, *ibid.* **85**, 844 (2000).
[5] S. Koshihara and H. Munekata, Phys. Rev. Lett. **78**, 4617 (1997).
[6] A. Melnikov *et al.*, Phys. Rev. Lett. **91**, 227403 (2003).
[7] A. V. Kimel *et al.*, Nature (London) **435**, 655 (2005).
[8] Y. Tokura, Rep. Prog. Phys. **69**, 797 (2006).
[9] *Colossal Magnetoresistive Oxides*, edited by Y. Tokura (Gordon and Breach, London, 1999).
[10] K. Miyano *et al.*, Phys. Rev. Lett. **78**, 4257 (1997); M. Fiebig *et al.*, Science **280**, 1925 (1998).
[11] From the oscillation period and the refractive index for the probe light, the speed of sound is evaluated to be 9 km/s, which is close to the value (6.5 km/s) reported in $Pr_{0.7}Ca_{0.3}MnO_3$ [M. Fiebig *et al.*, Appl. Phys. B **71**, 211 (2000); here, the value originally reported in this paper was corrected by a factor of 2].
[12] N. Takubo *et al.*, Phys. Rev. Lett. **95**, 017404 (2005).
[13] Y. Okimoto *et al.*, J. Phys. Soc. Jpn. **76**, 043702 (2007).
[14] Y. Tomioka and Y. Tokura, Phys. Rev. B **70**, 014432 (2004).
[15] T. Ogasawara *et al.*, Phys. Rev. B **68**, 180407(R) (2003).
[16] Recently, a laser-induced AF-F phase transition has been reported in the antiferromagnets that have the ferromagnetic phase as their high temperature phase. See J.-U. Thiele *et al.*, Appl. Phys. Lett. **85**, 2857 (2004); G. Ju *et al.*, Phys. Rev. Lett. **93**, 197403 (2004); K. Miyasaka *et al.*, Phys. Rev. B **74**, 012401 (2006).
[17] J. Nogués and I. K. Schuller, J. Magn. Magn. Mater. **192**, 203 (1999).